nature COMMUNICATIONS

OPEN

ARTICLE

Received 23 Dec 2010 | Accepted 12 Aug 2011 | Published 13 Sep 2011

DOI: 10.1038/ncomms1476

Information processing using a single dynamical node as complex system

L. Appeltant[1], M.C. Soriano[2], G. Van der Sande[1], J. Danckaert[1], S. Massar[3], J. Dambre[4], B. Schrauwen[4], C.R. Mirasso[2] & I. Fischer[2]

Novel methods for information processing are highly desired in our information-driven society. Inspired by the brain's ability to process information, the recently introduced paradigm known as 'reservoir computing' shows that complex networks can efficiently perform computation. Here we introduce a novel architecture that reduces the usually required large number of elements to a single nonlinear node with delayed feedback. Through an electronic implementation, we experimentally and numerically demonstrate excellent performance in a speech recognition benchmark. Complementary numerical studies also show excellent performance for a time series prediction benchmark. These results prove that delay-dynamical systems, even in their simplest manifestation, can perform efficient information processing. This finding paves the way to feasible and resource-efficient technological implementations of reservoir computing.

[1] Applied Physics Research Group (APHY), Vrije Universiteit Brussel, Pleinlaan 2, B-1050 Brussel, Belgium. [2] Instituto de Física Interdisciplinar y Sistemas Complejos, IFISC (UIB-CSIC), Campus Universitat de les Illes Balears, E-07122 Palma de Mallorca, Spain. [3] Laboratoire d'Information Quantique, CP 225, Université Libre de Bruxelles, Boulevard du Triomphe, B-1050 Bruxelles, Belgium. [4] Department of Electronics and Information Systems, Ghent University, St Pietersnieuwstraat 41, B-9000 Ghent, Belgium. Correspondence and requests for materials should be addressed to I.F. (email: ingo@ifisc.uib-csic.es).

Nonlinear systems with delayed feedback and/or delayed coupling, often simply put as 'delay systems', are a class of dynamical systems that have attracted considerable attention, both because of their fundamental interest and because they arise in a variety of real-life systems[1]. It has been shown that delay has an ambivalent impact on the dynamical behaviour of systems, either stabilizing or destabilizing them[2]. Often it is sufficient to tune a single parameter (for example, the feedback strength) to access a variety of behaviours, ranging from stable via periodic and quasi-periodic oscillations to deterministic chaos[3]. From the point of view of applications, the dynamics of delay systems is gaining more and more interest. While initially it was considered more as a nuisance, it is now viewed as a resource that can be beneficially exploited. One of the simplest possible delay systems consists of a single nonlinear node whose dynamics is influenced by its own output a time τ in the past. Such a system is easy to implement, because it comprises only two elements, a nonlinear node and a delay loop. A well-studied example is found in optics: a semiconductor laser whose output light is fed back to the laser by an external mirror at a certain distance[4]. In this article, we demonstrate how the rich dynamical properties of delay systems can be beneficially employed for processing time-dependent signals, by appropriately modifying the concept of reservoir computing.

Reservoir computing (RC)[5–10] is a recently introduced, bio-inspired, machine-learning paradigm that exhibits state-of-the-art performance for processing empirical data. Tasks, which are deemed computationally hard, such as chaotic time series prediction[7], or speech recognition[11,12], amongst others, can be successfully performed. The main inspiration underlying RC is the insight that the brain processes information generating patterns of transient neuronal activity excited by input sensory signals[13]. Therefore, RC is mimicking neuronal networks.

Traditional RC implementations are generally composed of three distinct parts: an input layer, the reservoir and an output layer, as illustrated in Figure 1a. The input layer feeds the input signals to the reservoir via fixed random weight connections. The reservoir usually consists of a large number of randomly interconnected nonlinear nodes, constituting a recurrent network, that is, a network that has internal feedback loops. Under the influence of input signals, the network exhibits transient responses. These transient responses are read out at the output layer via a linear weighted sum of the individual node states. The objective of RC is to implement a specific nonlinear transformation of the input signal or to classify the inputs. Classification involves the discrimination between a set of input data, for example, identifying features of images, voices, time series and so on. To perform its task, RC requires a training procedure. As recurrent networks are notoriously difficult to train, they were not widely used until the advent of RC. In RC, this problem is resolved by keeping the connections fixed. The only part of the system that is trained are the output layer weights. Thus, the training does not affect the dynamics of the reservoir itself. As a result of this training procedure, the system is capable to generalize, that is, process unseen inputs or attribute them to previously learned classes.

To efficiently solve its tasks, a reservoir should satisfy several key properties. First, it should nonlinearly transform the input signal into a high-dimensional state space in which the signal is represented. This is achieved through the use of a large number of reservoir nodes that are connected to each other through the recurrent nonlinear dynamics of the reservoir. In practice, traditional RC architectures employ several hundreds/thousands of nonlinear reservoir nodes to obtain good performance. In Figure 2, we illustrate how such a nonlinear mapping to a high-dimensional state space facilitates separation (classification) of states[14]. Second, the dynamics of the reservoir should be such that it exhibits a fading memory (that is, a short-term memory): the reservoir state is influenced by inputs from the recent past, but independent of the inputs from the far past. This property is essential for processing temporal sequences (such as speech) for which only the recent history of the signal is important. Additionally, the results of RC computations must be reproducible and robust against noise. For this, the reservoir should exhibit sufficiently different dynamical responses to inputs belonging to different classes. At the same time, the reservoir should not be too sensitive: similar inputs should not be associated to different classes. These competing requirements define when a reservoir performs well. Typically, reservoirs depend

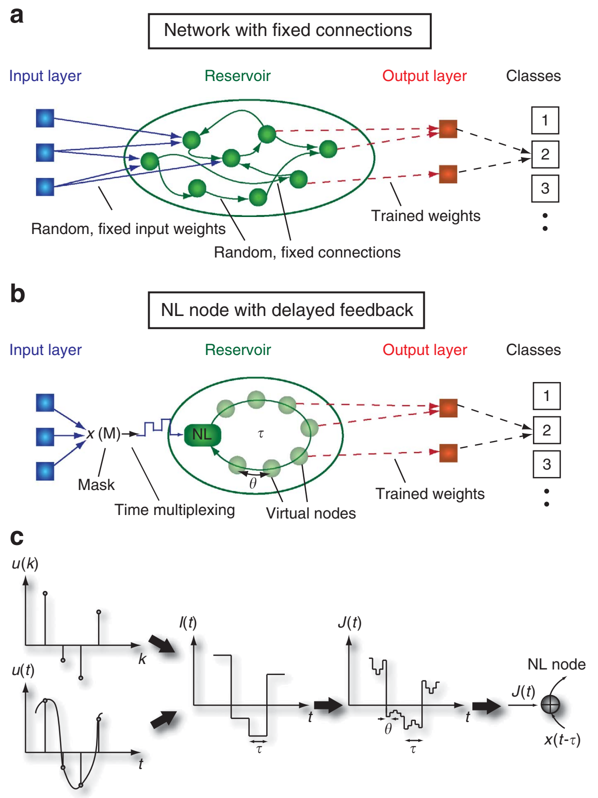

Figure 1 | Sketch of RC schemes. (**a**) Classical RC scheme. The input is coupled into the reservoir via a randomly connected input layer to the N nodes in the reservoir. The connections between reservoir nodes are randomly chosen and kept fixed, that is, the reservoir is left untrained. The reservoir's transient dynamical response is read out by an output layer, which are linear weighted sums of the reservoir node states $x_i(t)$. The output $\hat{y}(t)$ thus has the form $\hat{y}(t)=\Sigma_{i=1}^{N} w_i \cdot x_i(t)$. The coefficients w_i of the sum are optimized in the training procedure to best project onto the target classes. (**b**) Scheme of RC utilizing a nonlinear node with delayed feedback. A reservoir is obtained by dividing the delay loop into N intervals and using time multiplexing. The input states are sampled and held for a duration τ, where τ is the delay in the feedback loop. For any time t_0, the input state is multiplied with a mask, resulting in a temporal input stream $J(t)$ that is added to the delayed state of the reservoir $x(t-\tau)$ and then fed into the nonlinear node. The output nodes are linear weighted sums of the tapped states in the delay line given by $\Sigma_{i=1}^{N} w_i \cdot x(t-\frac{\tau}{N}(N-i))$. (**c**) Scheme of the input data preparation and masking procedure. A time-continuous input stream $u(t)$ or time-discrete input $u(k)$ undergoes a sample and hold operation, resulting in a stream $I(t)$ that is constant during one delay interval τ before it is updated. The random matrix M defines the coupling weights from the input layer to the virtual nodes. The temporal input sequence, feeding the input stream to the virtual nodes, is then given by $J(t)=M \times I(t)$.

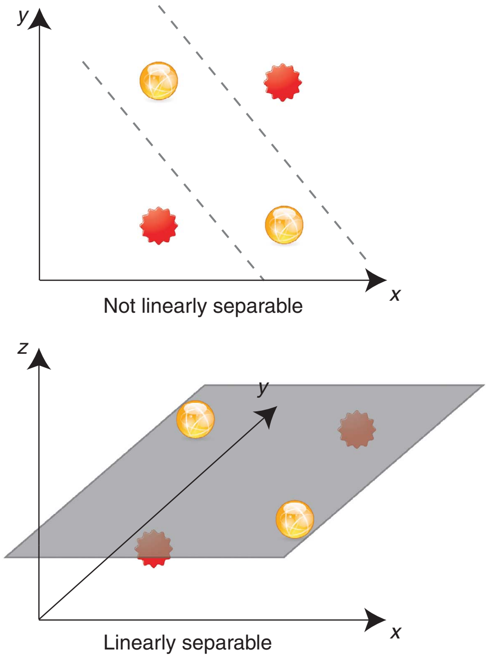

Figure 2 | Illustration of linear separability. It is well known that a non linear mapping from a small dimensional space into a high-dimensional space facilitates classification. This is illustrated in a simple example: In (**a**) a two-dimensional input space is depicted, in which the yellow spheres and the red stars cannot be separated with a single straight line. With a nonlinear mapping into a three-dimensional space, as depicted in (**b**), the spheres and stars can be separated by a single linear hyperplane. It can be shown that the higher dimensional the space is, the more likely it is that the data become linearly separable, see for example, ref. 14. RC implements this idea: the input signal is nonlinearly mapped into the high-dimensional reservoir state through the transient response of the reservoir. Furthermore, in RC the output layer is a linear combination with adjustable weights of the internal node states. The readout and classification is thus realized with linear hyperplanes, as in the figure.

on a few parameters (such as the feedback gain and so on) that must be adjusted to satisfy the above constraints. Experience shows that these requirements are satisfied when the reservoir operates (in the absence of input) in a stable regime, but not too far from a bifurcation point. Further introduction to RC, and in particular its connection with other approaches to machine learning, can be found in the Supplementary Discussion.

In this article, we propose to implement a reservoir computer in which the usual structure of multiple connected nodes is replaced by a dynamical system comprising a nonlinear node subjected to delayed feedback. Mathematically, a key feature of time-continuous delay systems is that their state space becomes infinite dimensional. This is because their state at time t depends on the output of the nonlinear node during the continuous time interval $[t-\tau, t[$, with τ being the delay time. The dynamics of the delay system remains finite dimensional in practice[15], but exhibits the properties of high dimensionality and short-term memory. Therefore, delay systems fulfil the demands required of reservoirs for proper operation. Moreover, they seem very attractive systems to implement RC experimentally, as only few components are required to build them. Here we show that this intuition is correct. Excellent performance on benchmark tasks is obtained when the RC paradigm is adapted to delay systems. This shows that very simple dynamical systems have high-level information-processing capabilities.

Results

Delay systems as reservoir. In this section, we present the conceptual basis of our scheme, followed by the main results obtained for the two tasks we considered: spoken digit recognition and dynamical system modelling. We start by presenting in Figure 1b the basic principle of our scheme. Within one delay interval of length τ, we define N equidistant points separated in time by $\theta = \tau/N$. We denote these N equidistant points as ‘virtual nodes’, as they have a role analogous to the one of the nodes in a traditional reservoir. The values of the delayed variable at each of the N points define the states of the virtual nodes. These states characterize the transient response of our reservoir to a certain input at a given time. The separation time θ among virtual nodes has an important role and can be used to optimize the reservoir performance. We chose $\theta < T$, with T being the characteristic time scale of the nonlinear node. With this choice, the states of the virtual nodes become dependent on the states of neighbouring nodes. Interconnected in this way, the virtual nodes emulate a network serving as reservoir (Supplementary Discussion). We demonstrate in the following that the single nonlinear node with delayed feedback performs comparably to traditional reservoirs.

The virtual nodes are subjected to the time-continuous input stream $\mathbf{u}(t)$ or time-discrete input $\mathbf{u}(k)$ which can be a time-varying scalar variable or vector of any dimension Q. The feeding to the individual virtual nodes is achieved by serializing the input using time multiplexing. For this, the input stream $\mathbf{u}(t)$ or $\mathbf{u}(k)$ undergoes a sample and hold operation to define a stream $\mathbf{I}(t)$ that is constant during one delay interval τ, before it is updated. Thus, in our approach, the input to the reservoir is always discretized in time, no matter whether it stems from a time-continuous or time-discrete input stream. To define the coupling weights from the stream $\mathbf{I}(t)$ to the virtual nodes we introduce a random (NxQ) matrix $\mathbf{M}$, in the following called mask (we recall that N is the number of virtual nodes). On carrying out the multiplication $\mathbf{J}(t_0) = \mathbf{M} \times \mathbf{I}(t_0)$ at a certain time t_0, we obtain a N dimensional vector $\mathbf{J}(t_0)$ that represents the temporal input sequence within the interval $[t_0, t_0 + \tau]$. Each virtual node is updated using the corresponding component of $\mathbf{J}(t_0)$. Alternatively, one can view $J(t)$ as a continuous time scalar function that is constant over periods, corresponding to the separation θ of the virtual nodes. Figure 1c illustrates the above input preparation and masking procedure. After a period τ, the states of all virtual nodes have been updated and the new reservoir state is obtained. Subsequently, $\mathbf{I}(t_0)$ is updated to drive the reservoir during the next period of duration τ. For each period τ, the reservoir state is read out for further processing. A training algorithm assigns an output weight to each virtual node, such that the weighted sum of the states approximates the desired target value as closely as possible (see Supplementary discussion). The training of the read-out follows the standard procedure for RC[5,7]. The testing is then performed using previously unseen input data of the same kind of those used for training.

To demonstrate our concept, we have chosen the widely studied Mackey–Glass oscillator[16]. The model of this dynamical system with its characteristic delayed feedback term, extended to include the external input $\mathbf{J}(t)$, reads

$$\dot{X}(t) = -X(t) + \frac{\eta \cdot [X(t-\tau) + \gamma \cdot J(t)]}{1 + [X(t-\tau) + \gamma \cdot J(t)]^p} \tag{1}$$

with X denoting the dynamical variable, $\dot{X}$ its derivative with respect to a dimensionless time t, and τ the delay in the feedback loop. The characteristic time scale of the oscillator, determining the decay of X in the absence of the delayed feedback term, has been normalized to $T = 1$. The parameters η and γ represent feedback strength and input scaling, respectively. The value of η we use guarantees that the system operates in a stable fixed point in the absence of external

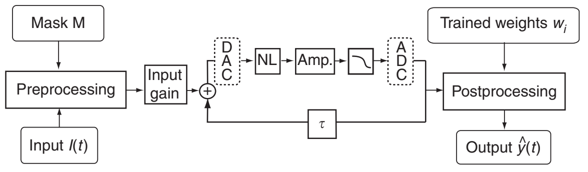

Figure 3 | Schematic of the experimental reservoir computer. The Mackey–Glass type nonlinear node is realized as in ref. 17. The time constant of the system is $T = 10$ ms. The delay loop is implemented digitally by means of Analog to Digital and Digital to Analog Converters (ADC and DAC). The preprocessing to create the input stream $\gamma J(t)$, with γ the adjustable input gain described in equation (1), and the postprocessing to create the output $\hat{y}(t)$ are also realized digitally. See Supplementary discussion for further details on the experimental implementation.

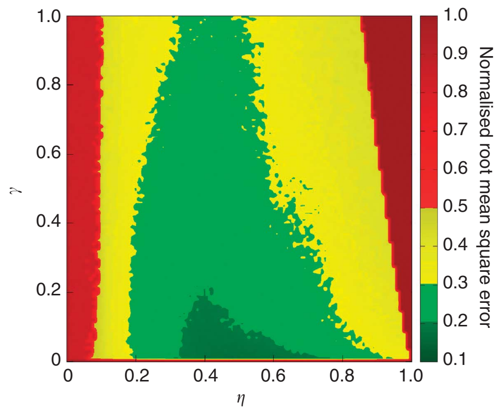

Figure 5 | Simulation results for the NARMA task. The two scanned parameters are γ (input scaling) and η (feedback strength). The exponent in equation (1) is set to $p = 1$. Other characteristics of the reservoir are as in Figure 4 ($\tau = 80$, $N = 400$, $\theta = 0.2$). The obtained performance for the NARMA-10 task, expressed as a normalized root mean square error, is encoded in colour.

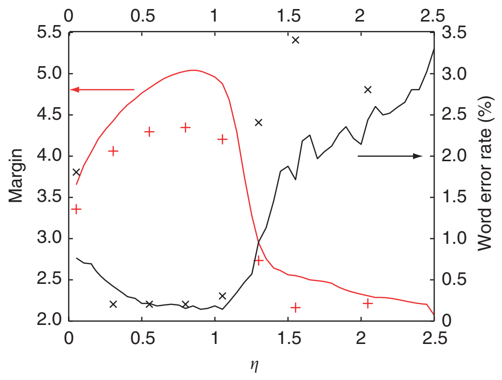

Figure 4 | Numerical and experimental results for spoken digit recognition. The y-axis on the left-hand side denotes the margin, whereas the y-axis on the right-hand side denotes the word error rate. The abscissa represents the parameter η. γ has been kept fixed at 0.5 and the exponent is set to $p = 7$. The delay time is set at $\tau = 80$, with $N = 400$ neurons of $\theta = 0.2$ separation. The red line represents results for the numerically obtained margin and the black line represents the numerically obtained word error rate. The red and black crosses denote the corresponding experimental results.

input ($\gamma = 0$). With input, however, the system might exhibit complex dynamics. The choice of the nonlinearity in equation (1) has two main advantages. First, it can be easily implemented by an analogue electronic circuit[17], which allows for fine parameter tuning[18]. This is the physical realization we have employed for the experimental demonstration (Fig. 3). Second, the exponent p can be used to tune the nonlinearity if needed. However, we expect other nonlinear functions to perform equally well.

Spoken digit recognition task. We now demonstrate by experiment and simulation, the capability of our single nonlinear delay-dynamical node to perform isolated spoken digits recognition. The isolated spoken digit recognition task, as introduced by Doddington and Schalk[19], is generally accepted as a benchmark speech recognition task. Our experimental realization has a Mackey–Glass nonlinearity with an exponent of $p = 7$ that is easily obtained with standard electronic components. We have verified through numerical simulations that a broad range of values of p yields similar results. The virtual node separation is set at $\theta = 0.2$ that offers optimal performance (Methods section), whereas the total number of virtual nodes is $N = 400$. The specifics of the training procedure are detailed in the Supplementary Discussion and the Methods section. As an example, Figure 4 depicts the experimentally and numerically obtained classification performance of unknown samples as a function of η for $\gamma = 0.5$, which has been chosen such that input and feedback signals are of the same order of magnitude. The classification performance is expressed in two ways: the word error rate (WER) that shows the percentage of words that have been wrongly classified, and the margin (distance) between the reservoir's best guess of the target and the closest competitor. It can be seen that an increase in margin corresponds to a decrease in WER. Our results show that there is a broad parameter range in η with good performance, with an optimum for both, margin and WER, around $\eta = 0.8$. Note that the performance breaks down when η approaches 1. This is expected as it corresponds to the threshold of instability of the MG oscillator when there is no input ($\gamma = 0$). At the optimum value of η, we obtain a WER as low as 0.2% in experiments and 0.14% in numerical simulations. This corresponds to only one misclassification in 500 words. These performance levels are comparable to or even better than those obtained with traditional RC composed of more than 1,200 nodes for which a WER of 4.3% was reported[11], with a reservoir of 308 nodes for which more recently a WER of 0.2% was obtained[12] and also with alternative approaches based on hidden Markov models that achieved a WER of 0.55% (ref. 20).

NARMA task as an example of dynamical system modelling. We now present results from numerical simulations demonstrating the computational capabilities of the single nonlinear delay-dynamical node for a second task, commonly used in RC literature: dynamical system modelling, in particular training the readout to reproduce a certain signal[21,22]. Specifically, we train the system to model the response to white noise of a discrete-time tenth order nonlinear auto-regressive moving average (NARMA) system, originally introduced in reference 23. The details of this benchmark are described in the Supplementary Discussion and in the Methods section. To quantify the performance of the reservoir, the normalized root mean square error (NRMSE) of the predicted value versus the value obtained from the NARMA model is used. Up to now, the best performance reported in traditional RC for a reservoir of $N = 100$ nodes, is NRMSE $= 0.18$ (ref. 12). If the reservoir is replaced by a shift register that contains the input, the minimal NRMSE is 0.4. NRMSE values below this level require a nonlinear reservoir. We have chosen a nonlinear exponent of $p = 1$, resulting in a weak nonlinearity that allows for longer memory as compared with the previously used value of $p = 7$ (Supplementary Discussion). Figure 5

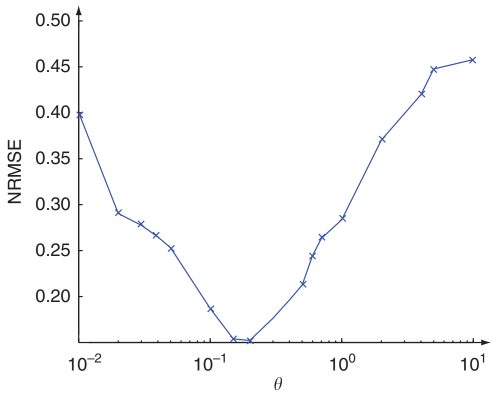

Figure 6 | Performance of NARMA task as a function of node separation. Plot of the normalized NRMSE for the NARMA-10 task (simulations) versus the separation θ of the virtual nodes. Parameters are: $\eta=0.5$, $\gamma=0.05$, $p=1$, $\tau=400\ \theta$.

depicts our numerical results in the $\gamma-\eta$ plane. A large region with NRMSE < 0.2 (dark green) has been obtained. In Figure 6, we depict the NRMSE as a function of the virtual node separation θ. The optimal value lies around $\theta=0.2$. When θ is larger, there is not enough coupling between virtual nodes, and performance decreases. When θ is smaller, too much averaging causes decreased performance. The minimal normalized root mean square error is as low as NRMSE = 0.15. We therefore achieved comparable performance to conventional RC, but with a much simpler architecture.

Discussion

We have demonstrated, both in experiment and simulation, that a simple nonlinear dynamical system subject to delayed feedback can efficiently perform information processing. As a consequence, our simple scheme can replace the complex networks used in traditional RC. Moreover, to the best of our knowledge, this experiment represents the first hardware implementation of RC with results comparable to those obtained with state-of-the-art digital realizations (Supplementary Discussion).

To get good performance with our system, a number of parameters need to be adjusted. These include the feedback gain η, the input gain γ, the delay time τ, the separation of virtual nodes in the delay line θ, the type of nonlinearity (in our case the exponent p of the MG system), and the choice of input mask. These parameters have analogues with similar parameters used in traditional RC: feedback gain and input gain have similar roles to spectral radius and input scaling; the delay time τ is related to the number of nodes and the separation of the virtual nodes to the sparsity of the interconnection matrix; the type of nonlinearity can also be varied in traditional RC and so on. As demonstrated here, some of the parameters can vary significantly around certain optimal values and still yield very good results. As experience with systems such as ours grows, we expect–as in traditional RC–that good heuristics on what parameter values to use will emerge. We expect that delay reservoirs can be realized that are, within some restrictions, versatile for different tasks. Moreover, owing to their much simpler hardware implementation, specifically optimized solutions for certain tasks could make sense. From a fundamental point of view, the simplicity of our architecture should facilitate gaining a deeper understanding of the interplay of dynamical properties and reservoir performance.

Besides the fundamental aspect of understanding information processing capabilities of dynamical systems, our architecture also offers practical advantages. The reduction of a complex network to a single hardware node facilitates implementations enormously, because only few components are needed. Nevertheless, the use of delay dynamical systems implies certain constraints, because the feeding of the virtual nodes is carried out serially, in contrast to the parallel feeding of the nodes in traditional RC. This serial feeding procedure results in a slow-down of the information processing, compared with parallel feeding. This potential slow-down is compensated for by the much simpler hardware architecture of the reservoir, and by the fact that the read-out can be taken at a single point of the delay line. These simplifications will enable ultra-high-speed implementations, using high-speed components that would be too demanding or expensive to be used for many nodes. In particular, realizations based on electronics or photonics systems should be feasible using this simple scheme, including real-time processing capabilities. Moreover, we expect that compromises can be found concerning speed, performance and memory capacity by extending the concept to network motifs of delay-coupled elements. Ultimately, a novel information-processing paradigm might emerge.

Methods

Spoken digit recognition task. In the spoken digit recognition task, the input dataset consists of a subset of the NIST TI-46 corpus[24] with ten spoken digits (0–9), each one recorded ten times by five different female speakers. Hence, we have 500 spoken words, all sampled at 12.5 kHz. The input $\mathbf{u}(k)$ (with k the discretized time) for the reservoir is, in this case, a set of 86-dimensional state vectors (channels) with up to 130 time steps. Each of these inputs represents a spoken digit, preprocessed using a standard cochlear ear model[25]. To construct an appropriate target function, ten linear classifiers are trained, each representing a different digit of the dataset. The target function is -1 if the spoken word does not correspond to the sought digit, and $+1$ if it does. For every target, the time trace is averaged in time and a winner-takes-all approach is applied to select the actual digit.

To eliminate the impact of the specific division of the available data samples between regularization, training and testing, we used n-fold cross-validation. This means that the entire process of regularization, training and testing is repeated n times (with $n=20$) on the same data, but each time with a different assignment of data samples to each of the three stages. The reported performances are the mean across these n runs.

For the spoken digit recognition task, the mask consists of a random assignment of three values: 0.59, 0.41 and 0. The first two values have equal probability of being selected, whereas the third one is more likely to be selected. Using a zero mask value implies that some nodes are insensitive to certain channels, thus avoiding averaging of all the channels.

NARMA10 task. The NARMA10 task is one of the most widely used benchmarks in RC. It was introduced in[21], and used in many other publications in the context of RC, for instance in references 23,26. For the NARMA10 task, the input $u(k)$ of the system consists of scalar random numbers, drawn from a uniform distribution in the interval [0, 0.5] and the target $y(k+1)$ is given by the following recursive formula

$$y_{k+1}=0.3y_k+0.05y_k\left[\sum_{i=0}^{9}y_{k-i}\right]+1.5u_ku_{k-9}+0.1. \qquad (2)$$

The input stream $J(t)$ for the NARMA10 test is obtained from u_k according to the procedure discussed in the manuscript. For the regularization, training and test of the dynamical system modelling task, we used 4 samples with a length of 800 points each and twofold cross-validation. The input scaling for the mask consists of a random series of amplitudes of 0.1 and -0.1. The input signal, multiplied with the mask and the input scaling factor γ, feeds the Mackey-Glass node as in equation (1). The importance of the parameters γ, the feedback strength η, and the separation between virtual nodes θ, has been discussed above. In particular, θ has a crucial role. In Figure 6, we show the numerically obtained performance of the Mackey–Glass system for the NARMA10 test when scanning θ. The optimal point is found for virtual node separations of $\theta=0.2$, in units of the characteristic time scale of the nonlinear node. For shorter separations, too much averaging takes place and the Mackey–Glass system does not respond to the external input. For larger separations, the connectivity among virtual nodes is lost and, consequently, also the memory with respect to previous input. For node separations $\theta>3$, the NRMSE reaches a level of 0.4, which is the performance of a shift-register.

References

1. Erneux, T. *Applied Delayed Differential Equations* (Springer Science + Business Media, 2009).
2. Schöll, E. & Schuster, H. G. *Handbook of Chaos Control* (2nd edn , Wiley-VCH, 2008).

3. Ikeda, K. & Matsumoto, K. High-dimensional chaotic behavior in systems with time-delayed feedback. *Physica* **D29**, 223–235 (1987).
4. Fischer, I., Hess, O., Elsässer, W. & Göbel, E. High-dimensional chaotic dynamics of an external cavity semiconductor laser. *Phys. Rev. Lett.* **73,** 2188–2191 (1994).
5. Jaeger, H. The 'echo state' approach to analyzing and training recurrent neural networks. *Technical Report GMD Report* **148**, German National Research Center for Information Technology (2001).
6. Maass, W., Natschläger, T. & Markram, H. Real-time computing without stable states: a new framework for neural computation based on perturbations. *Neural Comput.* **14,** 2531–2560 (2002).
7. Jaeger, H. & Haas, H. Harnessing nonlinearity: predicting chaotic systems and saving energy in wireless communication. *Science* **304,** 78–80 (2004).
8. Verstraeten, D., Schrauwen, B., D'Haene, M. & Stroobandt, D. An experimental unification of reservoir computing methods. *Neural Netw.* **20,** 391–403 (2007).
9. Buonomano, D. V. & Maass, W. State-dependent computations: spatiotemporal processing in cortical network. *Nat. Rev. Neurosci.* **10,** 113–125 (2009).
10. Maass, W., Joshi, P. & Sontag, E. Computational aspects of feedback in neural circuits. *PLOS Comput. Biol.* **3,** 1–20 (2007).
11. Verstraeten, D., Schrauwen, B., Stroobandt, D. & Van Campenhout, J. Isolated word recognition with the liquid state machine: a case study. *Inform. Process. Lett.* **95,** 521–528 (2005).
12. Verstraeten, D., Schrauwen, B. & Stroobandt, D. Reservoir-based techniques for speech recognition. In *Proceedings of IJCNN06*, International Joint Conference on Neural Networks, 1050–1053 (2006).
13. Rabinovich, M., Huerta, R. & Laurent, G. Transient dynamics for neural processing. *Science* **321,** 48–50 (2008).
14. Cover, T. Geometrical and statistical properties of systems of linear inequalities with applications in pattern recognition. *IEEE Trans. Electron.* **14,** 326–334 (1965).
15. Le Berre, M., Ressayre, E., Tallet, A., Gibbs, H. M., Kaplan, D. L. & Rose, M. H. Conjecture on the dimensions of chaotic attractors of delayed-feedback dynamical systems. *Phys. Rev. A* **35,** 4020–4022 (1987).
16. Mackey, M. C. & Glass, L. Oscillation and chaos in physiological control systems. *Science* **197,** 287–289 (1977).
17. Namajunas, A., Pyragas, K. & Tamasevicius, A. An electronic analog of the Mackey-Glass system. *Phys. Lett. A* **201,** 42–46 (1995).
18. Sano, S., Uchida, A., Yoshimori, S. & Roy, R. Dual synchronization of chaos in Mackey-Glass electronic circuits with time-delayed feedback. *Phys. Rev. E* **75,** 016207 (2007).
19. Doddington, G. & Schalk, T. Speech recognition: turning theory to practice. *IEEE Spectrum* **18,** 26–32 (1981).
20. Walker, W. *et al. Sphinx-4: A Flexible Open Source Framework for Speech Recognition* (Technical Report, Sun Microsystems, 2004).
21. Jaeger, H. Adaptive nonlinear system identification with echo state networks: in *Advance in Neural Information Processing Systems* (eds Becker, S., Thrun, S., Obermayer, K.) Vol 15, 593–600 (MIT Press, 2003).
22. Steil, J. In *Lecture Notes in Computer Science* Vol **3697**, 43–48 (Springer, 2005).
23. Atiya, A. F. & Parlos, A. G. New results on recurrent network training: unifying the algorithms and accelerating convergence. *IEEE T. Neural Netw.* **11,** 697–709 (2000).
24. Texas Instruments-Developed 46-Word Speaker-Dependent Isolated Word Corpus (TI46), September 1991, NIST Speech Disc 7-1.1 (1 disc).
25. Lyon, R. F. A computational model of filtering, detection, and compression in the cochlea. *Proc. IEEE-ICASSP'82*, vol. 7, 1282–1285 (1982).
26. Rodan, A. & Tino, P. Minimum complexity echo state network. *IEEE T. Neural Netw.* **22,** 131–144 (2011).

Acknowledgements
We thank the members of the PHOCUS consortium and the members of the IAP Photonics@Be for helpful discussions and I. Veretennicoff and G. Verschaffelt for careful reading of our manuscript. Stimulating discussions are acknowledged with Jan Van Campenhout by I.F. and J.Dan., and with Yvan Paquot and Marc Haelterman by S.M. This research was partially supported by the Belgian Science Policy Office, under grant IAP P6-10 'photonics@be', by FWO and FRS–FNRS (Belgium), MICINN (Spain) under projects FISICOS (FIS2007-60327) and DeCoDicA (TEC2009-14101) and by the European project PHOCUS (EU FET-Open grant: 240763). L.A. and G.VdS. are a PhD Fellow and a Postdoctoral Fellow of the Research Foundation-Flanders (FWO).

Author contributions
I.F., C.R.M., S.M., J.Dan., B.S., G.VdS., M.C.S. and J.Dam. have contributed to development and/or implementation of the concept. M.C.S. performed the experiments, partly assisted by L.A. and supervised by C.R.M. and I.F. L.A. performed the numerical simulations, supervised by G.VdS. and J.Dan. All authors contributed to the discussion of the results and to the writing of the manuscript.

Additional information
Supplementary Information accompanies this paper at http://www.nature.com/naturecommunications

Competing financial interests: The authors declare no competing financial interests.

Reprints and permission information is available online at http://npg.nature.com/reprintsandpermissions/

How to cite this article: Appeltant, L. *et al.* Information processing using a single dynamical node as complex system. *Nat. Commun.* 2:468 doi: 10.1038/ncomms1476 (2011).

Information processing using a single dynamical node as complex system

Supplementary Information

L. Appeltant[1], M.C. Soriano[2], G. Van der Sande[1], J. Danckaert[1] , S. Massar[3], J. Dambre[4], B. Schrauwen[4], C.R. Mirasso[2], I. Fischer[2,*]

1 Applied Physics Research Group (APHY),Vrije Universiteit Brussel, Pleinlaan 2, B-1050 Brussel, Belgium

2 Instituto de Física Interdisciplinar y Sistemas Complejos, IFISC (UIB-CSIC), Campus Universitat de les Illes Balears, E-07122 Palma de Mallorca, Spain

3 Laboratoire d'Information Quantique, CP 225, Université Libre de Bruxelles, Boulevard du Triomphe, B-1050 Bruxelles, Belgium

4 Department of Electronics and Information Systems, Ghent University, St. Pietersnieuwstraat 41, B-9000 Ghent, Belgium

Supplementary Figures

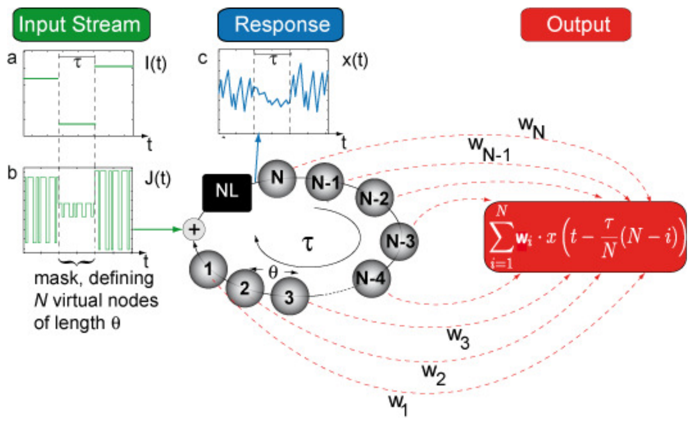

Supplementary Figure S1: Schematic representation of reservoir computing with a delayed feedback system and a single nonlinear node. The discrete input stream ***u****(k)* is transformed into a piecewise continuous function *I(t)* using a sample and hold procedure. Three time steps of length *τ* are represented in panel (a). This input is multiplied by the mask function *M(t)*. The mask function is piecewise constant over interval θ and periodic over period *τ*. In the present case the mask function is taken to be a binary function. The resulting function *J(t)=M(t)I(t)* is represented in panel (b) for 3 time steps. The sum *x(t-τ)+γ J(t)* drives the nonlinear node, where γ is an adjustable parameter. The response of the nonlinear node is a complex function x(t) depicted in panel (c). Finally, a linear combination of the values of the *N* virtual nodes is taken to obtain the output. The only parameters which are optimised in this procedure are the input gain γ, the degree of nonlinearity of the nonlinear node (typically depending on a single parameter), the separation θ of the nodes, and the output weights w_i .

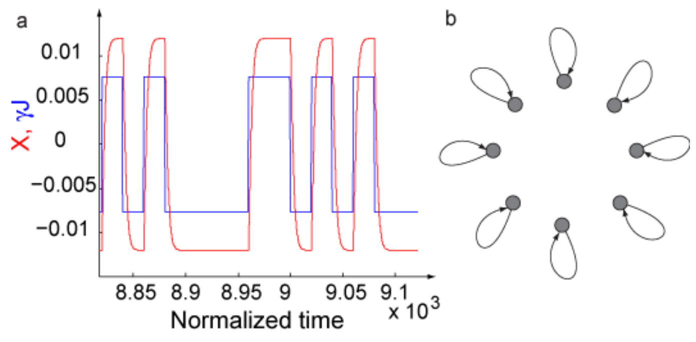

Supplementary Figure S2: Input time trace for large θ and corresponding interaction graph (a) Input time trace $\gamma \cdot J(t)$ (blue) and oscillator output *x(t)* (red) of our system when the time scale T of the Mackey-Glass system is much smaller than the separation θ of the virtual nodes T<<θ. Here we choose T/θ=0.05. The values on both the x- and y-axis are dimensionless. The mask M(t) takes two possible values. For this choice of parameters, the system rapidly reaches a state that is independent of previous inputs. In this regime the system behaves like *N* independent nodes, each of which is coupled only to itself at the previous time step, as schematised by the interaction graph in panel (b).

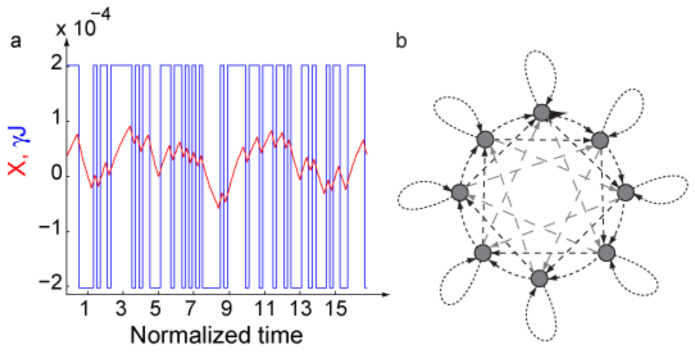

Supplementary Figure S3: Input time trace for small θ and corresponding interaction structure (a) Time trace of input γJ(t) (blue) and oscillator output *x(t)* (red) of our system when the time scale *T* of the Mackey-Glass system and the separation *θ* of the virtual nodes satisfy *T/θ=5 (This is the same plot as in Fig. 5)*. The values on both the x- and y-axis are dimensionless. The mask *M(t)* takes two possible values. In this case the system does not have the time to reach an asymptotic value. Therefore, the dynamics of the nonlinear node couples neighboring virtual nodes, as schematised by the interaction structure in panel (b).

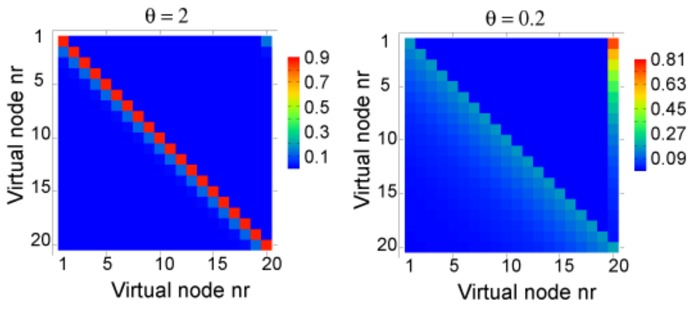

Supplementary Figure S4: Interaction graphs for large and small θ Interaction graphs for different virtual node separation where we plot the coefficients Ω_{ni} and Δ_{ji} of eq. S18 as a matrix using colour coding. For large values of θ (left), the diagonal elements are significantly larger than all others, but when θ decreases (right), the exponential tail of the off-diagonal elements and the also the connection to the last virtual node of the previous input step become dominant.

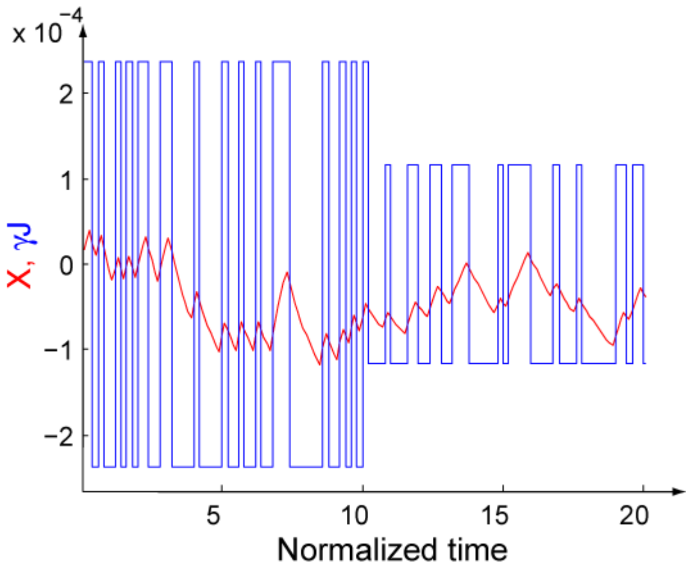

Supplementary Figure S5: Time trace NARMA10 task Time trace of the input stream and the corresponding response of the Mackey-Glass node for the optimal parameters for the NARMA10 task (η = 0.5, γ = 0.01, p = 1 and τ = 80 (400 nodes of 0.2 time units separation)). The blue line represents the input *J(t)* with imprinted input mask, multiplied by the input scaling γ. The red line shows the Mackey-Glass output *x(t)*. The values on both the x- and y-axis are dimensionless. As input mask, a random series of amplitudes of 0.1 and -0.1 are used.

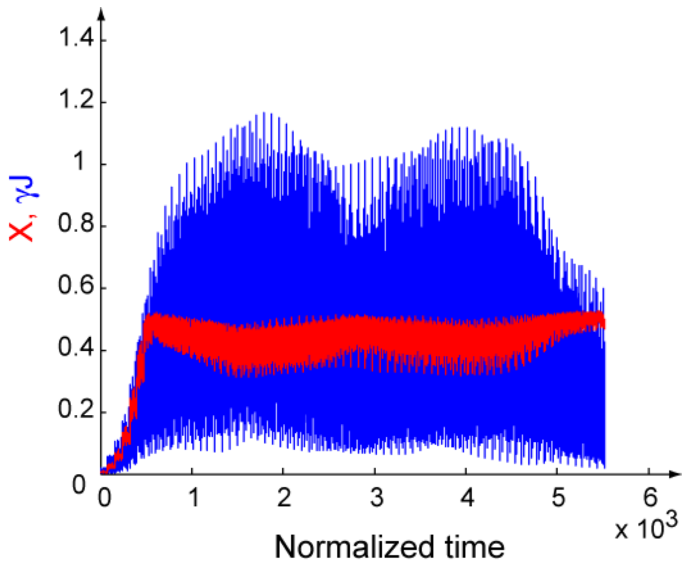

Supplementary Figure S6: Time-trace of the input stream and the corresponding response of the nonlinear node in the case of spoken digit recognition, represented over the duration of one spoken digit The input with imprinted input mask is multiplied by the input scaling γ and is represented by the blue line. The red line denotes the oscillator output. Parameters: $\eta = 0.8$, $\gamma = 0.5$, $p = 7$ and $\tau = 80$ with 400 nodes of 0.2 time units separation. The values on both the x- and y-axis are dimensionless.

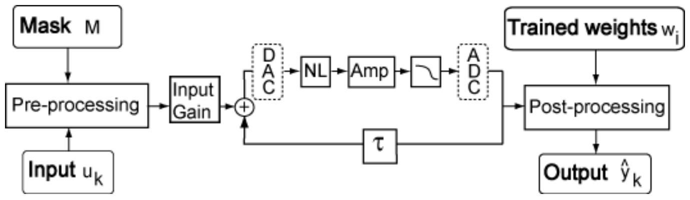

Supplementary Figure S7: Schematic representation of the experiment The Mackey Glass system is realised by a nonlinearity (NL), and amplifier (Amp), a low pass filter, and a delay. DAC and ADC, Digital to Analog Converter and Analog to Digital Converter respectively. The input gain block corresponds the parameter γ, while the amplification block corresponds to η.

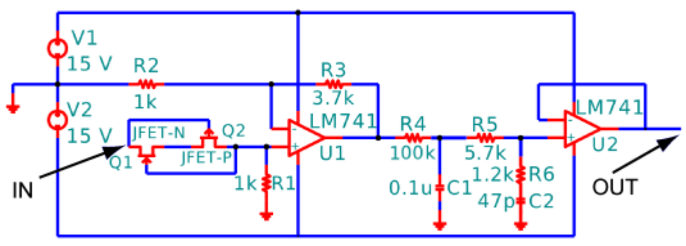

Supplementary Figure S8: Schematic representation of the hardware node Two FET transistors, one n-channel (Fairchild 2N5457) and one p-channel (Fairchild 2N5460) generate the nonlinear function itself. An amplifier (LM741) provides the desired magnification factor and two RC-circuits allow to set the time constant of the circuit. R1 = 507Ω, R2 = 1kΩ, R3 = 3.7kΩ, R4 = 100kΩ, R5 = 5.7kΩ, R6 = 1.2kΩ, C1 = 0.1μF, C2 = 47pF.

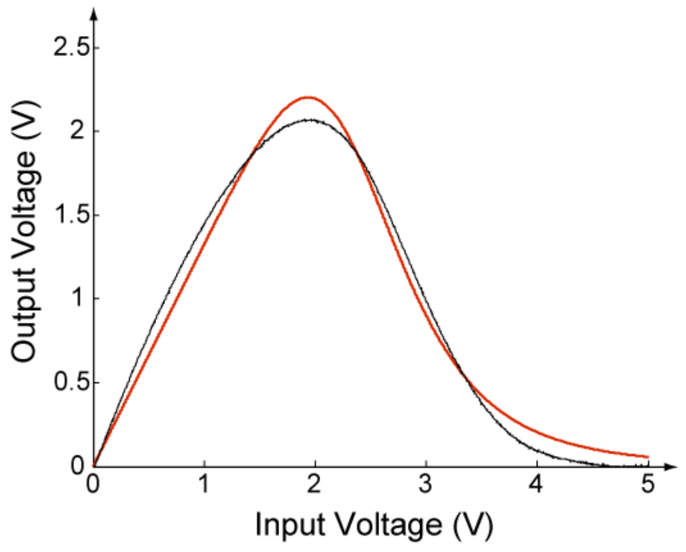

Supplementary Figure S9: Fitting of experimental transfer function Experimental transfer function (black) compared to a fit using the Mackey-Glass equation (red). Fit parameters correspond to C = 1.33, b = 0.4 and p = 6.88 (eq. S20).

Supplementary Discussion

Different perspectives on Reservoir Computing

Reservoir computing (RC) is a powerful method recently introduced in the field of machine learning. In hard classification or prediction tasks, it often outperforms other state-of-the-art approaches. For instance, RC improves prediction of chaotic dynamics by three orders of magnitude over previous methods [7]. Even more it won an international financial time series forecasting competition [27]. Concerning speech recognition, (isolated digit recognition), using the benchmark described in section 'Specific aspects of the benchmark tests', the word error rate was decreased from the previous best of 0.6% to 0.2% [12], while for the Japanese vowel benchmark the test error rate was brought to zero (previous best 1.8%) [28].

RC can be approached from different points of view and can therefore be linked to various fields of research.

From the viewpoint of machine learning, the techniques used in RC are related to those implemented in support vector machines, originally introduced by Vapnik [29]. Support vector machines have proven to be able to attain state-of-the-art performance on a number of tasks. They also rely on a mapping of a low-dimensional input onto high-dimensional states. The main difference to RC lies in the exact realisation of the high-dimensional mapping. While in RC the mapping is explicit - the dynamical response resulting in the reservoir states - , in support vector machines a technique called the kernel trick is employed [30]. The hyperplanes that separate two input classes in the high dimensional feature space are calculated by defining cross products in terms of a kernel function. A second difference is that in reservoir computing the mapping onto feature space is explicitly temporal. This is implemented by reservoirs exhibiting fading memory.

From the viewpoint of neuroscience, RC aims at mimicking, in a reductionist scheme, how our brain does information processing. In this context, RC assumes that the neurons are embedded in a randomly-connected complex network whose intrinsic activity is modified by external stimuli. The persistent neuronal network activity makes the information processing of a given stimulus occur in the context of the response to previous excitations. The generated network activity is then projected into other cortical areas that interpret or classify the outputs. It was this bio-inspired view that motivated one of the original RC concept (Liquid State Machine) [6].

From a dynamical systems point of view, the reservoir can be regarded as a complex dynamical system that operates optimally in a certain dynamical regime. Three basic properties, linked to the dynamical properties of the network [6], should be fulfilled for a network to perform as reservoir. Firstly, different inputs should be mapped onto different reservoir states. This is generally referred to as the *separation property*. Secondly, reservoir states that are only slightly different should be mapped onto identical targets. If not, noise would suffice to map identical inputs onto different target values. This is called the *approximation property*. Finally, *fading memory* is desired. In many tasks, the information is stored in the temporal behaviour of the input (e.g. speech recognition). It does not suffice to process the present input values, also previous values have to be taken into account. Usually, only recent inputs are relevant while those from the far past do not need to be taken into account. These three properties can be realised by the dynamical system, provided that the system resides in a proper dynamical regime. When the system operates in a chaotic regime, it is highly sensitive to small input variations and therefore has very good separation properties. The separation might, however, become so high that the approximation property no longer holds. In the reservoir community it is often claimed that the edge of chaos is an optimal operating point, since it offers a compromise between a stable system, with good approximation properties and fading memory, and a chaotic system, with excellent separation capability. More generally, the edge of stability, where the system goes from an ordered regime to another regime (oscillatory or chaotic), has been identified as appropriate operating point. This can be understood by noting that when a constant input is fed into the reservoir, most likely the target function will also be a constant. In case the system does not reside in a fixed point, but operates, e.g., in the oscillatory regime, a fluctuating reservoir state would need to be mapped onto a constant target, which is difficult to achieve with the linear training algorithm used in RC.

This viewpoint, relating RC to complex dynamics, suggests that RC can be implemented in a wide variety of physical systems, provided that separation, approximation and fading memory properties are fulfilled. This has led to a few proof-of-principle demonstrations using different systems such as a bucket of water [31], the cerebral cortex of a cat [32], a VLSI chip [33], or an array of semiconductor optical amplifiers [34] (the latter only in simulation). However, in all these implementations the tasks performed have been rather simple and the performances did not reach those of digital implementations.

Reservoir computing is not only of conceptual interest. Indeed because of its flexibility, RC represents an alternative approach to building information processing machines. It could find applications in regimes, such as ultra-low energy or ultra-fast computing, which are inaccessible with standard electronics. However the first step before starting to address these issues is to show that analog RC can be efficiently implemented and can reach performances comparable to digital realisations. It is this important milestone which is reached in the present work.

Reservoir computing: general concepts

Different variants of RC have been investigated. All of these variants comprise two layers. The first layer is called *'the reservoir'* or *'the liquid'*. This layer consists of a randomly interconnected network of nonlinear nodes (sometimes referred to as neurons). The nodes are driven by random linear combinations of Q input signals, projecting the original input signal onto a high dimensional state space. The emerging reservoir state is given by the combined states of all the individual nodes. Unlike with traditional recurrent neural networks, the coupling weights in the reservoir are not trained. They are usually chosen in a random way, globally scaled in order for the network to operate in a certain dynamical regime. The second layer performs the readout. Due to the projection of the low-dimensional input data onto a high dimensional space, the readout can be efficiently done by linearly combining the states of the system. The training algorithm can thus be simplified drastically to a linear classifier.

The RC implementation proposed in this paper is closely related to echo state networks [7]. In echo state networks the node states at time step k are computed according to the following equation:

$$\boldsymbol{x}(k) = f\left(W_{res}^{res} \cdot \boldsymbol{x}(k-1) + W_{in}^{res} \cdot \boldsymbol{u}(k) + W_{out}^{res} \cdot \hat{\boldsymbol{y}}(k-1) + W_{bias}^{res}\right) \qquad \text{S1}$$

In this equation, $\boldsymbol{x}(k)$ is the ($Nx1$)-dimensional vector of node states, $\boldsymbol{u}(k)$ is the ($Qx1$)-dimensional input matrix and $\hat{\boldsymbol{y}}(k)$ the reservoir output value(s), all at time step *k*. The matrices W_{xxx}^{res} contain the (generally random) reservoir, input and feedback connection weights and random bias values. The weight matrices W_{res}^{res} are scaled by multiplicative factors $W_{xxx}^{res} \to \alpha_{xxx} W_{xxx}^{res}$ in order to get good performance. For the nonlinear function f, often a sigmoidal function, such as $f(x) = tanh(x)$ is chosen. In some cases, feedback from the output to the reservoir nodes is also included. This is not used in our approach, we nevertheless include it here for completeness.

In the most general formulation, the output is a weighted linear combination of the node states, a constant bias value and the input signals themselves.

$$\hat{\boldsymbol{y}}(k) = W_{res}^{out} \cdot \boldsymbol{x}(k) + W_{in}^{out} \cdot \boldsymbol{u}(k-1) + W_{out}^{out} \cdot \hat{\boldsymbol{y}}(k-1) + W_{bias}^{out} \qquad \text{S2}$$

Sometimes the previous value of the output is also taken into account, but in our approach we set W_{out}^{out} to zero.

In RC only the matrices W_{xxx}^{out} in equation S2 are optimised (trained) to minimize the mean square error between the calculated output values $\hat{\boldsymbol{y}}(k)$ and the required output values **y**(k). During the whole process, all weight matrices in equation S1 remain unchanged.

The determination of optimal weight values W_{xxx}^{out}, the process referred to as training, can be performed either in one-shot (offline) learning or by gradually adapting the weights (online learning). The former approach has been applied in our work. It consists of driving the reservoir with a sufficient number of input samples (either a single time trace, as for the NARMA task, or multiple short time traces as for the Spoken Digit Recognition task, see 'Specific aspects of the benchmark tests') and recording the node states for each time step. For *N* nodes and *M* time steps, the result is a (*N*x*M*)-dimensional reservoir state matrix. To this matrix, we add a constant signal to generate the correct first moment of the required output signal. We will refer to the resulting ((*N*+1) x *M*) matrix as *S,* and to the concatenation of all readout weight matrices as *W,* being a *R* x (*N*+1) matrix, where *R* is the number of outputs. ***y*** designates the *R* x *M* matrix corresponding to the desired output. The aim is to minimize the mean square error $\left\|WS - \boldsymbol{y}\right\|^2$. This can be obtained by choosing

$$W = \left(\boldsymbol{y}\, S^{\dagger}\right)^{T} \qquad \text{S3}$$

Here † denotes the Moore-Penrose pseudo-inverse, which allows to avoid problems with ill-conditioned matrices.

After the training stage, the performance of the system is evaluated by applying previously unseen input signals to the reservoir (the testing stage).

In order to avoid overfitting to the training data, regularisation is commonly used, either by adding some Gaussian noise to the node states during training, or by using so-called *Tikhonov regularisation* or *ridge regression*, which minimizes $\left\|WS - \boldsymbol{y}\right\|^2 + \left\|\lambda W\right\|^2$ instead. The second term serves the purpose of keeping the weights as small as possible, while still minimizing the error. Regularisation complicates the training because the parameter λ needs to be optimized first, using yet another data set than the ones used in training and testing. In our paper, ridge regression was used.

For the reader interested in a more in-depth presentation of reservoir computing, we refer to the recent review articles [35,36,37].

Delayed feedback systems as reservoirs

Delayed feedback systems have been extensively studied in the nonlinear dynamics community, see e.g. [1]. The typical evolution equation for a delayed feedback system, such as used in the present work, is

$$\dot{\boldsymbol{x}}(t) = F\left(\boldsymbol{x}(t), \boldsymbol{x}(t-\tau)\right) \qquad \text{S4}$$

F describes a dynamical system, therefore an intrinsic time scale T is present in addition to the delay time τ. The role of these timescales will be discussed later.

Delayed feedback can have a significant impact on the dynamical behaviour of systems. It can e.g. lead to characteristic instabilities, induce synchronisation between subsystems, or also lead to stabilisation. Delayed feedback also implies that the phase space of the system becomes mathematically infinite dimensional, because its state is defined by the continuous function ***x****(s)* in the interval $t-\tau < s \leq t$. The delay induces many degrees of freedom, providing an explicit mapping from temporal to spatial information in a high-dimensional space [38].

In the present work we show how, in the context of RC, one can use systems with delayed feedback to drastically increase the available dimensions, even when only a single nonlinear node is used. This is done by exploiting both the present system's state and those of the past as *computing states*. Thus we replace the spatial multiplexing of usual RC (wherein multiple nonlinear nodes act in parallel) by time multiplexing in which a single nonlinear node processes the computing states sequentially.

To this end the delay interval is divided into N pieces of length $\theta=\tau/N$, their endpoints representing nodes. We refer to these nodes as virtual, because they are simply a delayed version of the output of the hardware node.

Contrary to the case of classical reservoirs, where the input vector at a certain time is injected in parallel to all nodes, in our system the input vector is fed to the nodes in a serial manner. We now outline this *masking procedure*, schematised in Supplementary Figure S1, see also Figure 1 (c) in the main text.

First, we sample and hold the input for a duration of τ (see Supplementary Figure S1(a)). The resulting function $I(t)$ is related to the continuous input signal $\boldsymbol{u}(k)$ by

$I(t)=\boldsymbol{u}(k)$ for $\tau k \le t < \tau(k+1)$ S5

Second, in order to break the symmetry between the N nodes, we multiply $I(t)$ by a mask function $M(t)$. This mask function is a piecewise constant function, constant over an interval of θ and periodic, with period τ. The values of the mask function during each interval of length θ are chosen independently at random from some probability distribution: $M(t)=W_{in,i}^{res}$ for $(i-1)\theta \le t \le i\theta$ and $M(t+\tau)=M(t)$, with $W_{in,i}^{res}$ random values. In terms of a 'classical' reservoir setup, the values of the mask function $M(t)$ correspond to the weights of the connection between the input layer and the reservoir layer. In equation S1 these weights were referred to as W_{in}^{res} .

When the input signal consists of a single channel, the values to be injected are given by

$$J(t)=I(t)\cdot M(t). \qquad \text{S6}$$

The function $J(t)$ is the product of the input and the mask function (Supplementary Figure S1(b)). When the input consists of Q values $I^j(t)$, we generate a separate mask $M^j(t)$ for each input j and subsequently they are all summed together. The value to be injected is then given by:

$$J(t)=\sum_{j=1}^{Q} I^j(t)\times M^j(t) \qquad \text{S7}$$

The resulting evolution equations are thus

$$\dot{x}(t)=F\left(x(t),x(t-\tau)+\gamma J(t)\right) \qquad \text{S8}$$

where γ is an adjustable parameter (usually referred to as input gain).

The final step when using the delay system as a reservoir computer is to construct the output using a (linear) perceptron so that every discrete input step $\boldsymbol{u}(k)$ is mapped onto a discrete target value $\hat{\boldsymbol{y}}(k)$ and this for every k. The reservoir state comprises the virtual node states, i.e. the values at the end of each interval θ. For the i^{th} virtual node the k^{th} discrete reservoir state is given by

$$x_k^i = x\left(k\tau-(N-i)\theta-\varepsilon\right) \qquad \text{S9}$$

with ε being a very small value compared to θ, which takes into account that the last simulated time step or the last experimental sample is taken. Thereafter a set of trained weights α_i for i = $1...N$ is used to calculate $\hat{\boldsymbol{y}}_{\boldsymbol{k}}=\sum_{i=1}^{N} w_i\, \boldsymbol{x}_k^i$, where $\hat{\boldsymbol{y}}(k)$ is the calculated approximation of the target function $\boldsymbol{y(k)}$

with $w_i = W^{out}_{res,i}$. The α_i are determined in such a way that the Normalised Root Mean Square Error, defined as

$$NRMSE = \sqrt{\frac{1}{M}\frac{\sum_{k=1}^{M}\left(\hat{y}_k - y_k\right)^2}{\sigma^2\left(y_k\right)}} \qquad \text{S10}$$

is minimized.

Notes on the Mackey-Glass model

Our starting point is the Mackey-Glass model introduced as a model of blood cell regulation [16], modified by an additional input *J(t')*

$$\dot{x}(t') = \frac{1}{T}\left[-x(t') + \frac{C\cdot\left[\alpha\cdot x(t'-\tau') + \beta\cdot J(t')\right]}{1+b^{p}\left[\alpha\cdot x(t'-\tau') + \beta\cdot J(t')\right]^p}\right], \qquad \text{S11}$$

with *C* being the coupling factor, *p* the exponent, *b* a nonlinearity coefficient, *T* the intrinsic timescale and τ the delay time. The factor *α* determines how much of the feedback signal is mixed with the input, while the factor *β* scales the magnitude of the input signal. The mixing of input and feedback signal happens just before the reinjection into the nonlinear node.

We have rescaled the variables and parameters in the previous equation to obtain the minimum number of significant parameters, as follows: $\eta = C\alpha$, $\gamma = b\beta$, X=bαx and $t = t'/T$, yielding

$$\dot{X}(t) = -X(t) + \frac{\eta\cdot\left[X(t-\tau) + \gamma\cdot J(t)\right]}{1+\left[X(t-\tau)+\gamma\cdot J(t)\right]^p}. \qquad \text{S12}$$

which is eq. (1) of the main text.

Time Scales

In the above delayed feedback system with external input we can identify three time scales: the separation of the virtual nodes *θ*, the delay time τ, and the timescale T of the Mackey-Glass system. We find that good performance occurs when the time scales are related by $\theta <\approx T << \tau$.

If $T << \theta$, the Mackey-Glass system reaches its steady state for each virtual node. In this case the reservoir state *x(t)* is only determined by the instantaneous value of the input *J(t)* and the delayed reservoir state *x(t- τ)*. There is no coupling between virtual nodes, and the dynamics of the system is too simple to perform well as reservoir. The behaviour in this case is illustrated in Supplementary Figure S2.

When $\theta<T$, the state *x(t)* of the system at time t depends on the states of the previous virtual nodes. The strength of this dependency is an exponentially decaying function of the separation of the virtual nodes. However, when *T/θ* is too large, the Mackey-Glass system is essentially not responding to the instantaneous value of the feedback and input, but only to the average taken over many previous nodes, which is not a good regime of operation either. Empirically we have found that for *N*=400 virtual nodes, the best choice is *T/θ*=5. This leads to significant coupling between virtual nodes, but without too much averaging. This regime is illustrated in **Supplementary Figure S3**.

Relation to Traditional Reservoir Computing

Here we establish a more formal link between the traditional formulation of RC given in 'Reservoir computing: general concepts' and the interconnection graphs presented in 'Time Scales'. In contrast to traditional reservoirs where all communication between nodes takes place from one discrete time step to another, in our concept interaction between nodes occurs through inertia of the nonlinear system and through the feedback line. For this reason, the interaction graphs shown in Supplementary Figure S2(b) and Supplementary Figure S3(b) do not quite correspond to the interconnection matrix W_{res}^{res} used in traditional reservoirs (see S1). In what follows, we will derive an approximate interconnection matrix W_{res}^{res} describing the coupling between virtual nodes processing information from different input time steps.

For simplicity of notation, in the following we normalise all times with respect to the intrinsic time scale of the nonlinear system *T*, that is we work in units where *T*=1.
Let us consider again the nonlinear equation for the Mackey-Glass node:

$$\dot{x}(t) = -x(t) + f\left(x(t-\tau), J(t)\right) \qquad \text{S13}$$

with

$$f\left(x(t-\tau), J(t)\right) = \frac{\eta\left[x(t-\tau) + \gamma J(t)\right]}{1 + \left[x(t-\tau) + \gamma J(t)\right]^p} \qquad \text{S14}$$

where *J(t)=M(t)I(t),* with *M(t)* the mask function. We recall that *I(t)* is constant over each segment with duration τ and equals *u(k)* over this segment.

In a linear approximation, assuming a constant value of *f(x(t-τ),J(t))* during the duration θ, solving the equation yields:

$$x(t) = x_0 e^{-t} + \left(1 - e^{-t}\right) f\left(x(t-\tau), J(t)\right) \qquad \text{S15}$$

where x_0 is the initial value at the beginning of each interval θ, i.e., the value for the previous virtual node. In particular, the values of the virtual nodes are given by S15 with *t* replaced by θ.

We now return to the discrete time of input signal ***u(k)*** The state of the ith virtual node (*i ∈[1,N])* is

reached after a time θ , denoted by $\boldsymbol{x}_{i,k}$. The input to virtual node *i* at time step *k* equals $w_{in,i}u_k$. (S15) can be written as:

$$\begin{aligned}
x_{1,k} &= x_{n,k-1}e^{-\theta} + \left(1-e^{-\theta}\right) f\left(x_{1,k-1}, w_{in,1}u_k\right) \\
&\dots \\
x_{i,k} &= x_{i-1,k}e^{-\theta} + \left(1-e^{-\theta}\right) f\left(x_{i,k-1}, w_{in,i}u_k\right) \\
&\dots \\
x_{n,k} &= x_{n-1,k}e^{-\theta} + \left(1-e^{-\theta}\right) f\left(x_{n,k-1}, w_{in,n}u_{n,k}\right)
\end{aligned} \qquad \text{S16}$$

where θ is the separation of the virtual nodes. This equation allows us to recursively compute each virtual node state at time step *k* only as a function of the input at the same time step *k* and virtual node states at time step *k-1*:

$$x_{i,k} = \Omega_{ni} x_{n,k-1} + \sum_{j=1}^{i} \Delta_{ji} f\left(x_{j,k-1}, w_{in,j} u_k\right) \qquad \text{S17}$$

with

$$\Omega_{ni} = e^{-i\theta},$$

$$\Delta_{ji} = \left(1 - e^{-\theta}\right) e^{-(i-j)\theta}. \qquad \text{S18}$$

This equation is our analogue of equation (S1), representing classical reservoirs and it explicitly describes the state coupling between consecutive time steps. However, it differs from traditional reservoirs because the nonlinear functions are applied to the states before the summation is taken. The interaction topology encoded in S17 is similar to that in the recently proposed cycle reservoir [26]. Supplementary Figure S4 illustrates this interaction topology by showing interaction strength matrices for two values of θ. The coefficients Ω_{ni} correspond to the values found in the last column, while the diagonal and off-diagonal elements are given by Δ_{ji}. In terms of traditional reservoirs, this can be related to W_{res}^{res} .

Specific aspects of the benchmark tests

In the following we provide more details on the procedures used to perform the two benchmark tests: NARMA10 and spoken digit recognition. As noted before, we work in units where the time constant of the nonlinear node is normalised to *T*=1. This corresponds to the experimental situation where the nonlinear node is fixed, and the delay τ and duration of virtual nodes θ can be adjusted.

NARMA10

The NARMA10 task is one of the most widely used benchmarks in reservoir computing. It was introduced in [23], and used in many other publications in the context of RC, for instance in [21] and [26].

For the NARMA10 task, the input *u(k)* of the system consists of scalar random numbers, drawn from a uniform distribution in the interval [0, 0.5] and the target *y(k+1)* is given by the recursion

$$y_{k+1} = 0.3 y_k + 0.05 y_k \left[\sum_{i=0}^{9} y_{k-i}\right] + 1.5 u_k u_{k-9} + 0.1. \qquad \text{S19}$$

In [21], for a reservoir of size *N*=100, the best performance reported is NRMSE=0.18 (eq. S10). If the reservoir is replaced by a shift register that contains the input, the minimal NRMSE is 0.4. NRMSE values below this level require a nonlinear reservoir.

We illustrate the input procedure, along with the response of the dynamical node, in Supplementary Figure S5. The time trace representing the input stream γJ(t) for the NARMA10 test is plotted in blue and the response of the nonlinear node is shown in red. The input mask consists of a random series of amplitudes of 0.1 and -0.1.The input signal, multiplied with the mask and the input scaling factor *γ*, is depicted together with the output of the Mackey-Glass node. Note how for this value of θ the Mackey-Glass system is in the transient regime for every node.

The importance of the parameters γ, *η* and *θ* is already discussed in the main paper. Note that the optimal parameters for the NARMA10 task are quite particular: the nonlinearity is weak (*p*=1), the input scaling is small (γ = 0.01), and the input mask is also small (random values of ± 0.1). This results in a better linear memory, which is crucial for this specific benchmark. Although, because of the memory requirements the node is close to linear, it still can significantly outperform a shift register that contains the input (for which NRMSE ≥ 0.4) and thus necessarily exploits the weak nonlinearities that are present. We have checked that this requires the inputs to be calculated with sufficiently high precision. These parameters and high precision are presently not accessible in our experiments.

Spoken digit recognition

The spoken digit recognition task, as introduced by Doddington and Schalk [19], is generally accepted as a basic speech recognition task in the RC community [11,12,19]. Also other approaches have used this test as a benchmark, one of them being the Sphinx 4 engine [20] by Sun Microsystems.

The input dataset for the spoken digit recognition consists of a subset of the NIST TI-46 corpus[1] with ten spoken digits (0...9), each one recorded ten times by five different female speakers. Hence, we have 500 spoken words, all sampled at 12.5 kHz. The input for the reservoir is in this case a set of 86-dimensional state vectors with up to 130 time steps. Each of these inputs represents a spoken digit, preprocessed using a standard cochlear ear model [25]. To construct an appropriate target function, ten linear classifiers are trained, each representing another digit of the dataset. The target function is -1 if it does not correspond to the targeted digit and +1 if it does. For every target the time trace is averaged in time and a winner-takes-all approach is applied to select the actual digit. To indicate the performance of the reservoir on this benchmark, the error is expressed both as the word error rate and as the margin. The margin expresses 'the distance' between the reservoir's best guess and the second best guess. When the 10 linear classifiers are trained to be +1 or -1, the resulting output series are averaged over the entire sample and the classifier with the highest mean value is selected to be the best approximation of the +1. If the margin is very high, this implies that the classification is very clear and that no confusion is possible. When the margin is very low, there is almost no difference between the best and the second best guess. Note that even with a very low margin, in theory the word error rate could still go down to 0%. However, both in simulation and experiment, we observe a clear correlation between margin and word error rate.

In the case of speech recognition, to eliminate the impact of the specific division of the available data samples between regularisation, training and testing, we use n-fold cross validation. This means that the entire process of regularisation, training and testing is repeated n times on the same data, but each time with a different assignment of data samples to each of the three stages. The reported performances are the mean across these n runs. For experiment and modelling we used n=20, thus a 20-fold cross validation. In the modelling we additionally averaged over 6 of such runs.

In **Supplementary Figure S6** we illustrate input and response of the Mackey-Glass node for the spoken digit recognition task. Similarly to the NARMA10 test, the nonlinear oscillator exhibits a transient behaviour (red line) because of the fast alternating input signal (blue line). The mask consists of a random assignment of three values: 0.59, 0.41 and 0. The first two values have equal probability of being selected, while the third one is more likely to be selected. Using a zero mask value implies that some nodes are insensitive to certain channels, thus avoiding averaging of all the channels. The degree of nonlinearity is now much higher: $p = 7$. For the spoken digit recognition task memory is of less importance and more emphasis is put on nonlinear transformation. Hence the node can be much more nonlinear and it becomes possible to implement this experimentally.

This spoken digit benchmark was introduced in the Reservoir Computing community in [11] where a WER of 4.3% was reported for a reservoir of size 1232. In [12] a winner-takes-all approach was introduced, and WER of 0.2% was obtained for a reservoir of size 308. In [26] a WER rate of 1.3%, both for traditional and cycle reservoirs of size 200 is reported. Our experimental system has a WER of 0.2%. For comparison, using Hidden Markov Models, the Sphinx-4 system [20] reported a WER of 0.55% on the same data set.

[1] Texas Instruments-Developed 46-Word Speaker-Dependent Isolated Word Corpus (TI46), September 1991, NIST Speech Disc 7-1.1 (1 disc).

Notes on the electronic Mackey-Glass implementation

Our experimental implementation of reservoir computing, as used in the spoken digit recognition experiments, is shown in Supplementary Figure S7.

Following [17], the Mackey-Glass system is constructed according to the scheme depicted in Supplementary Figure S8**.** The circuit consists of four parts: the nonlinearity, an amplifier, a RC-filter and a buffer. The nonlinearity was constructed using two field effect transistors, one p-channel, and one n-channel. Both of them are coupled with the gate of each transistor connected to the source of the other, resulting in a transfer function that can be fitted to the Mackey-Glass equation. In Supplementary Figure S both the experimentally observed transfer curve and the fit to the Mackey-Glass equation are depicted. To fit the nonlinearity to the Mackey-Glass equation we use

$$X_{out} = \frac{C \cdot X_{in}}{1 + b^p \left(X_{in} \right)^p}. \qquad \text{S20}$$

he RC filter is used to determine the time constant of the system, which is 10 ms (R4·C1). Connected to the circuit of Supplementary Figure S8, we added a PC controlled A/D D/A converter (National Instruments 6025E, 200 kSamples/s, 12-Bit A/D conversion). The delay line and the combination with the external input are both implemented digitally in the PC via LabView code. The continuously acquired data are delayed for a time corresponding to the feedback time. The input stream ***u(k)*** is converted into the function *J(t)* by imprinting the mask. Finally, the sum of external input *J(t)* and delayed output of the circuit are fed into the nonlinearity (FET transistors).

Supplementary References

27. http://www.neural-forecasting-competition.com/NN3/index.htm
28. Jaeger, H., Lukosevicius, M, Popovici, D., and Siewert, U.. Optimization and applications of echo state networks with leaky-integrator neurons. *Neural Networks*, 20(3), 335–352 (2007).
29. Vapnik, V.N., *The nature of statistical learning theory*. Statistics for engineering and information science. Springer, second edition (1999).
30. Aizerman, M., Braverman, E. And Rozonoer, L., Theoretical foundations of the potential function method in pattern recognition learning. *Automation and Remote Control*, **25**(6), 821-837 (1964).
31. Fernando, C., and Sojakka, S., Pattern Recognition in a Bucket, *Lecture Notes in Computer Science*, Volume 2801/2003, 588-597, DOI: 10.1007/978-3-540-39432-7_63 (2003).
32. Nikolic, D., Haeusler, S., Singer, W., and Maass, W., Temporal dynamics of information content carried by neurons in the primary visual cortex. *In Proc. of NIPS*, Advances in Neural Information Processing Systems, MIT Press **19,** 1041-1048 (2007).
33. Schürmann, F., Meier, K., Schemmel, J., Edge of Chaos Computation in Mixed-Mode VLSI - A Hard Liquid, *in proceedings of Advances in Neural Information Processing Systems* **17** [Neural Information Processing Systems, NIPS 2004, December 13-18, 2004, Vancouver, British Columbia, Canada]
34. Vandoorne, K., Dierckx, W., Schrauwen, B., Verstraeten, D., Baets, R., Bienstman, P., and Van Campenhout, J., "Toward optical signal processing using Photonic Reservoir Computing," *Opt. Express* 16, 11182-11192 (2008).
35. Legenstein, R.A. and Maass, W., Edge of chaos and prediction of computational performance for neural microcircuit models. *Neural Networks*, 323-333 (2007).
36. Lukoševičius, M., Jaeger, H., Reservoir computing approaches to recurrent neural network training, *Computer Science Review*, **3,** No. 3, 127-149 (2009).
37. Hammer, B., Schrauwen, B., Steil, J., Recent advances in efficient learning of recurrent networks; Brugge: d-facto; 2009. p. 213-226. In Proceedings of European Symposium on Artificial Neural Networks (ESANN 2009).

38. Giacomelli, G., Meucci, R., Politi, A., Arecchi, F.T., Defects and Spacelike Properties of Delayed Dynamical Systems, *Phys. Rev. Lett.* **73**, 1099 (1994).